



SCIENTIFIC OASIS

Decision Making: Applications in Management and Engineering

Journal homepage: www.dmame-journal.org
ISSN: 2560-6018, eISSN: 2620-0104

DECISION MAKING:
APPLICATIONS IN
MANAGEMENT AND
ENGINEERING

Designing a Log-Logistic-Based EWMA Control Chart Using MOPSO and VIKOR Approaches for Monitoring Cardiac Surgery Performance

Amir Nasiri Pour¹, Amir Azizi^{1,*}, Ayub Rahimzadeh², Mohammad Javad Ershadi³, Masoomeh Zeinalnezhad⁴

¹ Department of Industrial Engineering, Science and Research Branch, Islamic Azad University, Tehran, Iran

² Department of Industrial Engineering, Kermanshah Branch, Islamic Azad University, Kermanshah, Iran

³ Iranian Research Institute for Information Science and Technology (IRANDOC), Tehran, Iran

⁴ Department of Industrial Engineering, West Tehran Branch, Islamic Azad University, Tehran, Iran

ARTICLE INFO

Article history:

Received 7 August 2023

Received in revised form 27 November 2023

Accepted 30 November 2023

Available online 11 December 2023

Keywords: Exponentially weighted moving average; Risk-adjustment; Accelerated failure time; Multi-objective particle swarm optimization; PSO; Vlekraterijumsko KOMpromisno Rangiranje; VIKOR.

ABSTRACT

This study aims to develop a risk-adjusted Exponentially Weighted Moving Average (EWMA) control chart for computer-based performance monitoring in cardiac surgery. Patients have distinct risk factors that impact the surgical process before it even begins. As a result, risk adjustment is carried out utilizing the Accelerated Failure Time (AFT) model to consider these factors. Before using the risk-adjusted EWMA chart, the optimal parameter design should be established, considering the required statistical and economic factors. A model for Multi-Objective Decision Making (MODM) with multiple assignable causes has been proposed to accomplish this. The model is solved using a two-stage methodology based on the Multi-Objective Particle Swarm Optimization (MOPSO) method and the Vlekraterijumsko KOMpromisno Rangiranje (VIKOR) method. An actual case study for cardiovascular patients has been undertaken to demonstrate the performance and effectiveness of the suggested model. The multi-objective and pure economic models have been thoroughly compared. The economic model with statistical constraints and the multi-objective model have also been compared again. The findings suggest that the multi-objective design of the risk-adjusted EWMA chart exhibits higher statistical performance in both cases against a small augment in cost.

1. Introduction

Monitoring health systems has become an essential part of modern health care, which improves the quality of surgical and other medical services and leads to the proper decision-making in a healthcare system. Control charts are the foremost practical monitoring tools in healthcare, which are used to detect shifts in process parameters [1]. However, one of their best types is the EWMA control chart, which performs better for statistical monitoring and detecting small shifts in healthcare. When this chart is used for process monitoring, four parameters must be determined: sample size, sampling interval, control limit, and parameter designed to detect a specific shift in the

* Corresponding author.

E-mail address: azizi@srbiau.ac.ir

<https://doi.org/10.31181/dmame712024903>

chart optimally. Choosing a set of these parameters is called control chart design [2]. Control chart design has many economic and statistical aspects. To monitor the mean of a process with a single assignable cause, Duncan [3] established the first economic design. The design parameters were chosen such that the estimated cost of each product was kept to a minimum. His cost model included sampling costs, expenses related to out-of-control alarms, expenses of detecting and correcting assignable causes, and expenses of receiving a defective product from the customer. After that, other researchers carried out influential studies, and until today, many articles have been published about the economic design of control charts. Another famous model for economic design was proposed by Lorenzen and Vance [4], which is more flexible than Duncan's model. In this model, the process can stop or continue its work while searching to discover and correct the assignable cause. In the following, Serel [5] worked on the economic design of EWMA control charts based on Taguchi's loss function. Lu and Huang [6] investigated the statistically constrained economic design of maximum double EWMA control charts based on loss functions. Xue *et al.* [7] proposed an economical design for a residuals EWMA control chart incorporating variable sampling intervals and sample sizes.

However, the economic design of control charts may lead to poor statistical properties, making managers' decisions to use control charts doubtful. Statistical properties include the probability of type I and II errors or the in-control and out-of-control Average Run Length (ARL) [8]. Saniga [9] introduced the Economic-Statistical Design (ESD) by adding type I and type II errors as constraints to Duncan's economic model to improve the statistical properties of a control chart designed with economic models. The ESD helps to achieve the desired economic and statistical properties simultaneously. After that, many works were done in this field. Niaki *et al.* [10] compared the ESD and economical design of EWMA control charts and introduced a particle swarm optimization method to solve it. Amiri *et al.* [11] created an EWMA control chart with a scenario-based robust economic and ESD to consider economic and statistical criteria and uncertainty. Katebi and Pourtaheri [12] examined the ESD of the Poisson EWMA control charts for nonconformity monitoring. Lee *et al.* [13] scrutinized the ESD of the variable sampling interval Poisson EWMA chart.

Monitoring hospital outputs and clinical processes has become essential for health systems. Patients in these systems form a heterogeneous community due to having different preoperative characteristics such as age, gender, diabetes, blood pressure, etc. Therefore, the probability of death of each patient after surgery depends not only on the surgeon's skill but also on the preoperative characteristics of each patient. Therefore, monitoring and evaluation of surgical performance should be adjusted based on these characteristics. This process is called risk adjustment [14]. It is important that it is only possible to diagnose the appropriateness or inappropriateness of surgical quality by considering risk adjustment. If risk adjustment is not considered, control charts lose their efficiency as a quality improvement tool. Se-go *et al.* [15] presented a procedure to control censored surgery data using a novel risk-adjusted control chart. Mohammadian *et al.* [16] suggested phase I risk-adjusted geometric control charts to monitor healthcare systems. A risk-adjusted-based monitoring procedure has been addressed by Begun *et al.* [17] to detect shifts in the revision rates of hip replacement. Kim *et al.* [18] utilized a risk-adjusted control chart to monitor the surgical outcomes and set the training plan for laparoscopic pancreaticoduodenectomy. Yeganeh *et al.* [19] applied a risk-adjusted method to monitor patients' mortality rates based on an evolutionary artificial neural network.

To the best of our knowledge and based on the careful literature review, the design of risk-adjusted charts to control patients' treatment process and recovery has not been conducted. The present study intends to develop a multi-objective ESD model for risk-adjusted EWMA control charts. There are different methods to solve the proposed model, among which the MOPSO and the VIKOR

are the two most potent optimization methods. MOPSO is an advantageous evolutionary algorithm to achieve optimal solutions from the multi-objective model [20]. Therefore, this algorithm is utilized to find non-dominated solutions for the suggested model. Then, VIKOR is applied to classify the prioritization of the non-dominated solution [21]. VIKOR has been extensively used to solve multi-criteria problems in management and economy areas, including assessing the challenges to renewable energy technologies [22] and the performance assessment of circular economy [23]. Thus, by defining appropriate alternatives, VIKOR can also be utilized in multi-objective economic-statistical design. Therefore, this paper aims to assess and reach the optimal parameters in the multi-objective design of the risk-adjusted EWMA control chart in the treatment process and recovery of patients with both statistical and economic considerations using MOPSO and VIKOR methods.

The paper is structured in the manner described below. The overview of the risk-adjusted EWMA control chart is covered in Section 2. Section 3 of the risk-adjusted EWMA discusses the risk-adjusted EWMA's economic design. The MOESD paradigm is further explained in Section 4. Section 5 describes the MOPSO and VIKOR algorithms that are used to solve the model. Section 6 shows a factual example involving cardiovascular patients to illustrate how the proposed approach should be used. The comparisons of the proposed and existing models are covered in Section 7. Section 8 offers concluding remarks and a conclusion.

2. The Overview of the Risk-adjusted EWMA Scheme

The Surgical and recovery process of cardiovascular patients is considered when it is planned to monitor the mortality rate. In healthcare systems, patients have distinct and unrivaled health backgrounds, evaluated commonly by risk factor scores. The risk factor score is a well-known method for determining the probability of patient death from a specific treatment process [24]. According to the definition of this score, it is clear that the performance of a patient's surgical process depends on these preoperative risks. Hence, the control chart must be risk-adjusted to have a capable monitoring procedure. The risk-adjusted monitoring scheme is a significant issue in the healthcare system that has received much attention. To quickly identify shifts in the mortality rate, a monitoring approach based on patient survival time adjusted for the impact of risk factors is required.

Additionally, the duration of survival is a variable with a predictable character. Two critical characteristics of reliability make the monitoring of such data complicated. The first is that reliability data frequently adhere to location-scale and log-location-scale specific parametric distributions. The second problem is that capturing precise reliability data values is only sometimes possible for time and financial reasons. This issue forces one to consider the censoring mechanism as a different factor when working with reliable data. To tackle the problem of heterogeneity among patients, a regression model is required, which includes the use of covariates. The AFT model, a subset of survival analysis regression models, has been applied [25]. Therefore, it is interesting that censored survival times monitoring requires specific techniques. A vector of distribution parameters based on the AFT model will be depicted as $\Lambda_i = (\beta, x_i)$, where β signifies a vector of regression coefficients and x_i denotes risk factors for the patient i (a vector of covariates).

As previously indicated, the AFT regression model may simulate survival times using the parametric distributions from location-scale and log-location-scale families. The log-logistic distribution is among the most valuable and practical distributions among them. If the random variable of survival time is considered to follow a log-logistic distribution, the density function and survival function are expressed by:

$$f(y) = \frac{\Upsilon}{g} \left(\frac{y}{g}\right)^{\Upsilon-1} \left[1 + \left(\frac{y}{g}\right)^\Upsilon\right]^{-2}, \text{ and } S(y) = \left[1 + \left(\frac{y}{g}\right)^\Upsilon\right]^{-1} \quad (1)$$

in which, $g > 0$ is the scale parameter and $\Upsilon > 0$ is the shape parameter [15]. Based on what has been discussed for the AFT model, the scale parameter of the log-logistic distribution will be related to the unique risk factor (covariate). Doing so, the survival function is formed as follows:

$$S(y|x) = \left[1 + \left(\frac{y}{\exp(\beta_0 + \beta_1 x)}\right)^\Upsilon\right]^{-1} = \left[1 + \left(\frac{y}{g \exp(\beta_1 x_i)}\right)^\Upsilon\right]^{-1} \quad (2)$$

in which β_0 and β_1 represent regression model parameters. It is clear from the above equations that the scale parameter and the shape parameter are both included in the AFT model for the log-logistic distribution. It is noteworthy that the log-logistic distribution represents the mean survival time. As a result, a shift in the average survival time has the same meaning as a shift in the scale parameter, which is the shift for which the EWMA control chart was meant to work optimally. The risk-adjusted EWMA chart must be created and used when the AFT model has been properly constructed to consider preoperative risks about survival time.

A new patient score has been proposed in this study to provide a more accurate and easy-to-understand assessment of surgical outcome quality. This score called the area score, calculates the area under a patient's expected mortality distribution between zero and their actual survival time, taking into account both the observed and expected outcomes based on continuous measurement. This new score provides a more detailed and precise description of surgical outcome quality without adding complexity to its implementation or understanding. The area scores can then be used as control statistics in control charts for monitoring the surgical outcome quality in a risk-adjusted manner. The area score for each patient i who has surgery is given as s_i , and y_i is the value corresponding to the measured survival time. The anticipated result is determined by subtracting the expected mortality from 1. The equation is used to determine the likelihood that a patient will survive by utilizing the log-logistic survival function (Eq. (2)). The area score is defined as

$$s_i = \begin{cases} \int_0^{t_i} (1 - S_i(t)) dt & \left[\int_0^{t_i} \left(1 - \left[1 + \left(\frac{t_i}{g \exp(\beta_1 x_i)}\right)^\Upsilon\right]^{-1}\right) dt, \text{ if } 0 < y_i \leq c \right. \\ \left. 0 - (1 - S_i(t)) \right] & \left[0 - \left(1 - \left[1 + \left(\frac{t_i}{g \exp(\beta_1 x_i)}\right)^\Upsilon\right]^{-1}\right), \text{ otherwise} \right. \end{cases} \quad (3)$$

in which

$$t_i = \min(y_i, c) \quad (4)$$

Where c represents how long after surgery is right-censored [26], this work is planned to discover diminishing shifts in the mean survival periods according to the sensitive essence of healthcare systems and the high and irreversible cost of errors in patients' lives. We converted the area scores as follows for this purpose:

$$s_i = \left[\int_0^{t_i} (1 - S_i(t)) dt \right] = \left[\int_0^{t_i} \left(1 - \left[1 + \left(\frac{t_i}{\mathcal{G} \exp(\beta_1 x_i)} \right)^r \right]^{-1} \right) dt \right] \quad (5)$$

An effective patient survival time monitoring system combines the area score and the EWMA control chart. The statistic of this risk-adjusted EWMA chart (\mathbb{C}) is as a result:

$$\mathbb{C}_i = \Lambda s_i + (1 - \Lambda) \mathbb{C}_{i-1}, \quad 0 < \Lambda \leq 1, \quad (6)$$

The smoothing parameter Λ is a number between zero and one. The starting value \mathbb{C}_0 equals to the mean of patient scores from the in-control process. Liu *et al.* [27] demonstrated that a small Λ ($\Lambda = 0.005$) can be good at discovering a slight shift. Since an EWMA control chart for detecting decreasing shifts is presented, it is only necessary to consider a lower control limit (*LCL*). Consequently, the EWMA chart sets off an alarm that is out of control as soon as $\mathbb{C}_i < LCL$. Therefore, more investigation is required to identify the underlying causes, and remedial actions must be implemented to ensure a recovery.

3. The Economic Aspect on Healthcare Monitoring

The design parameters of the risk-adjusted EWMA control chart must be chosen to keep the cost of implementing the monitoring scheme to a minimum to consider the economic element of this chart. The risk-adjusted EWMA control chart's design parameters are:

- The sample size (n),
- Sampling interval (h),
- Lower control limit (*LCL*), and
- Defined coefficient for the best identification of a particular shift (ν).

To economically design the risk-adjusted EWMA chart, this study uses Lorenzen and Vance's [4] cost function with the property of numerous assignable causes. The period until the j^{th} assignable cause occurs is assumed to follow an exponential distribution, and the process starts under controlled conditions. Hospital costs and sample costs related to out-of-control patient treatments and expenses about assignable cause diagnosis and corrective action make up the total anticipated cost in a cycle for healthcare monitoring. Additionally, a cycle's expected length consists of three distinct components:

1. The anticipated time until an assignable cause occurs,
2. The time until an out-of-control signal is seen, and
3. The time it takes to identify the underlying cause and make the necessary changes to the process.

So, for the envisaged length of a cycle, given by:

$$Exp_T = \frac{1}{\sum_{j=1}^s \lambda_j} + \frac{\left[\sum_{j=1}^s \lambda_j \cdot [(h \cdot (ARL_1)_j) - \tau_j] \right]}{\sum_{j=1}^s \lambda_j} + \frac{\left[\sum_{j=1}^s \lambda_j \cdot (TI_j + TC_j) \right]}{\sum_{j=1}^s \lambda_j} \quad (7)$$

where λ_j denotes the rate of occurrence of the j^{th} assignable cause per hour, s indicates the number of assignable causes, and τ_j is the expected time of occurrence of the j^{th} assignable cause between the u^{th} and $u+1^{\text{st}}$ samples which is obtained as

$$\frac{1 - (1 + \lambda_j \cdot h) \cdot e^{-\lambda_j \cdot h}}{\lambda_j \cdot (1 - e^{-\lambda_j \cdot h})} \quad (8)$$

Moreover, T_{ij} and TC_j are the expected times to identify and repair the j^{th} assignable cause, respectively. Subsequently, the total expected cost of a cycle is equal to:

$$\begin{aligned}
 Exp_C = CE \cdot & \frac{1}{\sum_{j=1}^s \lambda_j} + \frac{\left[\sum_{j=1}^s \lambda_j \cdot [(h \cdot (ARL_1)_j) - \tau_j] \right]}{\sum_{j=1}^s \lambda_j} + \frac{\left[\sum_{j=1}^s \lambda_j \cdot (\gamma_{1j} T_{ij} + \gamma_{2j} TC_j) \right]}{\sum_{j=1}^s \lambda_j} \\
 & \frac{h}{\sum_{j=1}^s \lambda_j} \\
 & + \frac{\left[\sum_{j=1}^s \lambda_j \cdot CO_j \cdot (ARL_1)_j \right]}{\sum_{j=1}^s \lambda_j} + \frac{\left[\sum_{j=1}^s \lambda_j \cdot (CI_j + CC_j) \right]}{\sum_{j=1}^s \lambda_j}
 \end{aligned} \tag{9}$$

where CE represents the expenses associated with sampling for each patient; CO_j is the hospital's cost related to out-of-control treatment for each patient due to the j^{th} assignable cause, CI_j and CC_j are the costs to identify and fix the j^{th} assignable cause, respectively. Besides, $\gamma_{1j} = 1$ if the process continues during the identification, and $\gamma_{1j} = 0$ otherwise. $\gamma_{2j} = 1$ if the process continues during repairing time and $\gamma_{2j} = 0$ otherwise. Generally, the expected cost of the process expressed in unit time can be calculated as $Exp_A = Exp_C / Exp_T$. Subsequently, a multi-objective problem is presented in the next section to overcome the weak statistical characteristics of the economic design.

4. Economic and Statistical Design of risk-adjusted EWMA Monitoring Scheme

Multi-objective decision-making (MODM) intends to reach solutions in scenarios with several objectives that must be optimized simultaneously. MODM consists of constraints and inconsistent objectives related to mathematical programming procedures to solve problems [28]. As was already established, the main issue with the control charts' economic design is the need for the appropriate statistical characteristics. It should be emphasized that the probability of types I and II errors, the ARL_0 and ARL_1 , or the average time to signal when the process is under control ($ATS_0 = h \cdot ARL_0$) and average time to signal when the process is out of control ($ATS_1 = h \cdot ARL_1$) are statistical features. As a result, the ESD is created, and certain statistical restrictions need to be added to the pure economic model to achieve the desired statistical features. The statistical properties are improved compared to the pure economic design technique, although the predicted cost is slightly higher. As a result, the ESD model helps to increase the control chart's performance for identifying shifts.

Herein, the ESD model of the risk-adjusted EWMA chart is constructed to consider both the economic and statistical properties. The optimal design parameters in the proposed MODM model are selected to maximize the ATS_0 and $1/ATS_1$ and minimize the Exp_A cost function. Therefore, the proposed MODM design model for the risk-adjusted EWMA chart is formed as follows:

$$\begin{aligned}
 & Min \quad Exp_A(D) \\
 & Max \quad ATS_0(D) \\
 & Max \quad \left(\frac{1}{ATS_1(D)} = \frac{\lambda}{\sum_{j=1}^s \lambda_j ATS_{1j}(D)} \right) \\
 & s.t. \\
 & ATS_0(D) \geq ATS_0^L \\
 & ATS_{1j}(D) \leq ATS_1^U
 \end{aligned} \tag{10}$$

where a probable combination of design parameters is denoted by $D = (n, h, LCL, \nu)$. In addition, ATS_1^U and ATS_0^L refer to the upper and lower bound of out-of-control and in-control average time to signals, respectively. Hence, it is apparent that the MODM problem tries to optimize a set of conflicting objectives. The solution approach built on the combination of MOPSO and VIKOR for optimizing the multi-objective problem provided in Eq. (10) is described in more detail in the next section.

5. The Two-stage Solution Methodology

Several methods can be suggested to work out the given MOESD model. However, Pareto solutions are produced when numerous objectives are optimized concurrently. MOPSO, one of the most well-liked multi-objective evolution algorithms for resolving several issues, may be effectively applied to choose the optimal Pareto set. MOPSO has been used in some research on the control chart design to produce the ideal Pareto set, including the one presented by Tavana *et al.* [29]. Similarly, MOPSO is used in this study to solve the model shown in Eq. (10). However, applying this technique presents a difficulty since it frequently offers several options, and it might be challenging to select the most crucial solution from the optimal Pareto set. The VIKOR ranking and prioritizing tool for Pareto solutions is presented as a solution to this problem. To find the optimal solutions of the MODM model of the risk-adjusted EWMA control chart, a two-step solution approach based on MOPSO and VIKOR is proposed in this paper. To that aim, before presenting the VIKOR approaches, a quick introduction to MOPSO is given. It should be highlighted that the MATLAB (version R2016a) environment was used to assist the computations connected to the solution approach.

5.1 MOPSO

These algorithms aim to study a feasible area in search of non-dominated answers quickly. The effectiveness of four meta-heuristic algorithms when used to the ESD of charts was compared by Niaki *et al.* [10], who concluded that PSO is the most effective method for resolving their issue. As a result, the suggested MOESD model is solved using a MOPSO. The MOPSO algorithm is recommended when the PSO technique resolves the multi-objective optimization issue. The multi-objective optimization issue is complicated and contradictory and is currently under investigation. Fast convergence, outstanding robustness, and high dependability of MOPSO make it easier to find the local optimal value in multi-objective optimization problems [20]. The steps of the MOPSO algorithm are summarized as follows:

1. Specify the required parameters for MOPSO.
2. Randomly initialize population positions as the initial population.
3. Evaluate the fitness values for every position.
4. Identify non-dominated solutions and delete all dominated solutions simultaneously.
5. Update $pbest$ and $gbest$ for each particle, where $pbest$ represents a particle's best location and $gbest$ represents the position of all the particles together.
6. Calculate the velocity vector for each particle according to Eq. (11):

$$V_i(t+1) = wcV_i(t) + coe_1.r_1[pbest_i(t) - x_i(t)] + coe_2.r_2[gbest(t) - x_i(t)] \quad (11)$$

where $x_i(t)$ depicts the position of the i^{th} particle in the t^{th} iteration, wc is the weighting coefficient, coe_1 and coe_2 are the acceleration coefficients, and r_1 and r_2 are random variables ranging from 0 to 1.

7. Move the particles to the new positions according to the Eq. (12):

$$x(t+1) = x(t) + V(t+1) \tag{12}$$

8. Continue from step 3 until the termination requirement is met.

The risk-adjusted EWMA control chart's parameters in this study serve as the model's decision variables.

5.2 VIKOR

The VIKOR technique was developed to optimize complex problems using several criteria. The compromise ranking roster, compromise solution, and weight stability intervals for preference stability of the compromise solution created using the original weights are all included in this section. This approach concentrates on ranking and choosing from a list of possibilities when there are conflicting criteria. It recommends employing a multi-criteria ranking index built around a specific norm for an answer's "closeness" to the "ideal" response. The steps of the VIKOR method are summarized as follows [30]:

1. Establish the decision matrix,

After concluding the design alternatives and criteria, the decision matrix having an order of $M \times N$ is represented as:

$$D_{M \times N} = \begin{bmatrix} x_{11} & x_{12} & \dots & x_{1N} \\ x_{21} & x_{22} & \dots & x_{2N} \\ \vdots & \vdots & \dots & \vdots \\ x_{M1} & x_{M2} & \dots & x_{MN} \end{bmatrix} \tag{13}$$

A decision matrix element x_{ij} ($i = 1, 2, \dots, M$ and $j = 1, 2, \dots, N$) represents the actual measured value of the i^{th} alternative in terms of the j^{th} criteria when there are M choices and N criteria.

2. Specify the ideal and negative ideal solutions,

In ranking process, the ideal solution $(x_{ij})_{\max}$ and the negative ideal solution $(x_{ij})_{\min}$ are computed via Eq. (14) and Eq. (15):

$$\begin{cases} (x_{ij})_{\max} = \max[x_{ij}, i = 1, 2, \dots, M] \\ (x_{ij})_{\min} = \min[x_{ij}, i = 1, 2, \dots, M] \end{cases}, \quad \text{if } j \text{ is benefit criteria} \tag{14}$$

$$\begin{cases} (x_{ij})_{\max} = \min[x_{ij}, i = 1, 2, \dots, M] \\ (x_{ij})_{\min} = \max[x_{ij}, i = 1, 2, \dots, M] \end{cases}, \quad \text{if } j \text{ is not benefit criteria} \tag{15}$$

3. Calculate the utility measure and the regret measure,

Eq. (16) to Eq. (17) may be used to represent the utility measure ut_i and regret measure re_i values for each non-dominated solution:

$$ut_i = \sum_{j=1}^N \frac{\text{weight}_j [(x_{ij})_{\max} - x_{ij}]}{[(x_{ij})_{\max} - (x_{ij})_{\min}]}, \tag{16}$$

$$re_i = \max^x \text{ of } \left\{ \frac{\text{weight}_j [(x_{ij})_{\max} - x_{ij}]}{[(x_{ij})_{\max} - (x_{ij})_{\min}]} \right\}, \tag{17}$$

where the $weight_j$ is the weight of the j^{th} criteria. The weights are usually specified by the decision maker.

4. Calculate the VIKOR index,

The VIKOR index Ω_i is calculated using Eq. (18):

$$\Omega_i = \xi \left[\frac{ut_i - ut_i^-}{ut_i^+ - ut_i^-} \right] + (1 - \xi) \left[\frac{re_i - re_i^-}{re_i^+ - re_i^-} \right], \quad ut_i^+ = \max[ut_i, i = 1, 2, \dots, M], \quad (18)$$

$$ut_i^- = \min[ut_i, i = 1, 2, \dots, M], \quad re_i^+ = \max[re_i, i = 1, 2, \dots, M], \quad re_i^- = \min[re_i, i = 1, 2, \dots, M]$$

where, $\xi \in [0, 1]$ is a weight for the maximum value of utility and $(1 - \xi) \in [0, 1]$ is a weight of the individual regret. The value of ξ is usually taken as 0.5.

5. Rank the order of preference,

6. The best alternative option is the one with the smallest VIKOR index. The ranking is then maintained by the VIKOR index's ascending order.

7. Validate the ranking results based on the measure Ω_i ,

To do so, the following two conditions need to be satisfied:

Condition 1) Acceptable stability in decision-making: Alternative A^1 must also be ranked best by ut or/and re . A^1 is the alternative with the first position in the ranking list by Ω .

Condition 2) Acceptable advantage:

$$\Omega(A^2) - \Omega(A^1) \geq 1 / (M - 1) \quad (19)$$

A^2 is the alternative with second position in the ranking list by Ω and M is the number of alternatives.

A series of compromise solutions is provided if one of the prerequisites is not met, and they consist of:

- Alternative A^1 and A^2 if condition 1 is not satisfied, or
- Alternative A^1, A^2, \dots, A^n if condition 2 is not satisfied. A^n specified by Eq. (20) for maximum n .

$$\Omega(A^n) - \Omega(A^1) < 1 / (M - 1) \quad (20)$$

6. The Study of Cardiovascular Patients in Government Hospital

This section explores the implementation of the risk-adjusted EWMA monitoring scheme at a cardiovascular surgical center in the western region of Iran using its ESD (Imam Reza Hospital). The surgical treatment known as a coronary artery bypass graft (CABG) was selected for this case study, and information on 100 patients was collected throughout time. The dataset contains data on the date of admission, the primary care physician, the treatment regimen, the duration of survival, and the risk factor score. A weighted combination of each patient's preoperative risks makes up the risk factor score, considered the single covariate influencing survival time in this treatment technique. The preoperative risks for patients with cardiovascular conditions are listed in Table 1.

Table 1

The risk factors of patients utilized to calculate the influential variable

| Risk factors | Assigned weight |
|---|-----------------|
| Female gender | 6 |
| Age: 70 to 75 / 76 to 79 / 80 to ... | 2.5 / 7 / 11 |
| Diabetes | 3 |
| Hypertension | 3 |
| Morbid obesity: Over 1.5 times ideal weight | 1 |
| Congestive failure | 6 |
| COPD | 2.5 |
| Ejection fraction: < 30% / 30 to 49% | 8 / 6.5 |
| Left-main disease | 2.5 |
| Preoperative Intra-aortic balloon pump | 4 |
| Reoperation | 10 |
| Cardiogenic shock | 12 |
| Endocarditis, active | 6.5 |
| Tricuspid | 5 |
| Transmural acute myocardial infraction | 4 |
| Ventricular septal defect, acute | 12 |
| Ventricular tachycardia, ventricular fibrillation, aborted sudden death | 1 |
| Asthma | 1 |
| Endotracheal tube, preoperative | 4 |
| Idiopathic thrombocytopenic purpura | 12 |
| Pulmonary hypertension: mean pressure > 30 | 11 |
| Cirrhosis | 12.5 |
| Dialysis dependency | 13.5 |
| Renal failure, acute or chronic | 3.5 |
| Carotid disease | 2 |
| Peripheral vascular disease, severe | 3.5 |
| Blood products refused | 11 |
| Severe neurologic disorder | 5 |
| Percutaneous transluminal coronary angioplasty or catheterization | 5.5 |
| Substance abuse | 4.5 |

The log-logistic AFT model, as previously indicated, modifies the preoperative risks on patients' survival periods. The patients' survival rates were suppressed on the fourteenth day due to the laws and restrictions of Iran's Ministry of Health and Medical Education. The 14th day was chosen since it is the standard benchmark for clinical performance for cardiovascular patients at the government hospital, and patients typically have stable symptoms by then. Table 2 provides the computed risk factor scores and the patient survival rates.

Table 2
 The survival times and risk factor scores for cardiovascular patients

| Patient No. | Risk factors score | Survival time | Patient No. | Risk factors score | Survival time |
|-------------|--------------------|---------------|-------------|--------------------|---------------|
| 303569 | 22 | 14 | 304084 | 27 | 14 |
| 303597 | 16.5 | 14 | 304087 | 16.5 | 14 |
| 303599 | 52.5 | 3 | 304096 | 19.5 | 14 |
| 303600 | 14 | 14 | 304098 | 21 | 14 |
| 303605 | 14.5 | 14 | 304120 | 10 | 14 |
| 303609 | 11 | 14 | 304136 | 19 | 14 |
| 303620 | 20 | 14 | 304244 | 47 | 8 |
| 303624 | 33.5 | 14 | 304254 | 22 | 14 |
| 303626 | 17.5 | 14 | 304264 | 19 | 14 |
| 303634 | 16 | 14 | 304270 | 36 | 14 |
| 303645 | 11.5 | 14 | 304279 | 43.5 | 5 |
| 303652 | 11 | 14 | 304280 | 24 | 14 |
| 303670 | 16 | 14 | 304288 | 13.5 | 14 |
| 303672 | 10 | 14 | 304293 | 21 | 14 |
| 303673 | 27 | 14 | 304305 | 13 | 14 |
| 303687 | 32 | 14 | 304321 | 26 | 14 |
| 303711 | 29 | 14 | 304334 | 14 | 14 |
| 303732 | 16 | 14 | 304337 | 16.5 | 14 |
| 303754 | 23.5 | 14 | 304342 | 12.5 | 14 |
| 303755 | 11.5 | 14 | 304344 | 15 | 14 |
| 303905 | 11 | 14 | 304350 | 31 | 14 |
| 303908 | 7 | 14 | 304355 | 21.5 | 14 |
| 303927 | 10 | 14 | 304367 | 9 | 14 |
| 303932 | 18.5 | 14 | 304380 | 15 | 14 |
| 303936 | 39 | 11 | 304385 | 26 | 14 |
| 303938 | 11.5 | 14 | 304386 | 16 | 14 |
| 303942 | 23 | 14 | 304415 | 8 | 14 |
| 303953 | 24 | 14 | 304419 | 7 | 14 |
| 303959 | 19 | 14 | 304437 | 10 | 14 |
| 303962 | 22.5 | 14 | 304456 | 30.5 | 14 |
| 303964 | 25 | 14 | 304459 | 9 | 14 |
| 303969 | 20 | 14 | 304462 | 11 | 14 |
| 303972 | 11 | 14 | 304470 | 9 | 14 |
| 303995 | 29.5 | 14 | 304474 | 10.5 | 14 |
| 304001 | 37 | 14 | 304482 | 15 | 14 |
| 304008 | 10 | 14 | 304502 | 61 | 2 |
| 304020 | 28 | 14 | 304513 | 24.5 | 14 |
| 304024 | 26 | 14 | 304518 | 19 | 14 |
| 304028 | 21 | 14 | 304520 | 11.5 | 14 |
| 304040 | 14 | 14 | 304536 | 25 | 14 |
| 304041 | 10.5 | 14 | 304538 | 16 | 14 |
| 304065 | 38.5 | 14 | 304566 | 15.5 | 14 |
| 304071 | 43 | 6 | 304581 | 25 | 14 |
| 304072 | 20.5 | 14 | 304586 | 25 | 14 |
| 304073 | 13 | 14 | 304587 | 18.5 | 14 |
| 304077 | 37 | 14 | 304591 | 19 | 14 |
| 304078 | 13 | 14 | 304593 | 57 | 4 |
| 304081 | 28 | 14 | 304595 | 11 | 14 |
| 304082 | 34 | 14 | 304596 | 14 | 14 |
| 304083 | 27 | 14 | 304599 | 18 | 14 |

Initially, the information gathered from 100 patients was considered to create the proper distribution and calculate the parameter values. The findings indicated that a Gamma distribution with scale and shape parameters of 4.590 and 4.545 was present in the data corresponding to the risk factor score. The log-logistic AFT model's in-control parameters were then estimated via maximum likelihood estimation ($\vartheta = 8.0021$, $\Upsilon = 0.2400$ and $\beta_1 = 0.0194$). So, the survival function and the area score of the risk-adjusted EWMA are computed using Eq. (2) and Eq. (5).

Furthermore, the design parameters must be established to generate the risk-adjusted EWMA chart throughout the surgical process. This suggests that the risk-adjusted EWMA must have the optimal coefficient of descending shift following the proper lower limit to fulfill both the economic and statistical characteristics throughout the surgical procedure and post-operative recovery of cardiovascular patients. As mentioned earlier, the critical problem of surveillance patients in healthcare systems makes the value of n constant and equal to 1.

In addition, due to hospital rules and policies, a patient's case can be reviewed every 12 hours. Thus, the h value is also constant ($h = 12$). However, ν ranges from 0.01 to 0.2, and LCL ranges from -0.75 to -0.01. Consequently, the described MODM model is applied to choose the combination of parameters (LCL , ν) to reach the desired objectives of maximum statistical properties and the minimum expected cost. In the surgical and recovery process of cardiovascular patients, it was observed that two assignable causes that are medication errors and ventilator failure, happen with the rates of $\lambda_1 = 0.025h$ and $\lambda_2 = 0.005h$. When medication errors are the assignable cause, the patient's chance of survival decreases by around 90%, whereas the chance of survival decreases by about 95% when ventilator failure is the assignable cause.

Concerning filling out the risk factor questionnaire, conducting tests, and taking other steps to get risk factor score records, each patient's sample expenses amount to 2,000,000 Rials. 53,373,000 Rials are the expenditures incurred by the hospital in the out-of-control conditions brought on by medication errors. These costs cover check-ups, consultant, treatment, anesthesia, consumables, consumable medications, nursing services, ICU beds, and public beds. Similarly, the hospital was required to pay for check-ups, consultations, and consumable drugs, totaling about 2,393,000 Rials, due to the out-of-control conditions brought on by the assignable cause of the ventilator failure. The expenditures incurred by the hospital for the two assignable causes are shown in Table 3.

Table 3

The descriptions of the costs in the out-of-control situations corresponding to the incidence of the two assignable causes

| Action | The assignable cause related to medication errors | The assignable cause related to ventilator failure | Cost (in Rial) |
|---------------------------|---|--|----------------|
| Check-ups | * | * | 1,705,000 |
| Consultant | * | * | 208,000 |
| Anesthesia | * | | 684,000 |
| Public beds for 14 nights | * | | 20,240,000 |
| Consumable products | * | | 5,900,000 |
| Treatment | * | | 5,720,000 |
| Consumable drugs | * | * | 1,110,000 |
| ICU bed for 2 nights | * | | 15,244,000 |
| Nursing services | * | | 3,236,000 |

* symbol indicates that if an assignable cause occurs, the cost of action will be imposed on the hospital.

In addition, it takes five hours to identify the assignable cause of medication errors and the time required to convene a committee and look into the issue. Additionally, taking corrective action for

medication errors takes 2.5 hours on average. Similarly, it takes an expert in medical equipment around 4 hours to identify the reason for a ventilator failure and an average of 80 hours for a ventilator to be mended or replaced. About 20,000,000 Rials will be spent searching for the medication error-related assignable cause, while 16,000,000 Rials will be used to rectify medication errors. Researching ventilator failure to find the problems typically costs 14,500,000 Rials, and 15,000,000 Rials are being considered for ventilator repair or replacement. Table 4 lists the input parameters concerning the assignable causes that have been explored.

Table 4
 Input parameters values

| The assignable cause | Tl_j (Hours) | Tc_j (Hours) | CO_j (Rials) | Cl_j (Rials) | CC_j (Rials) | γ_{1j} | γ_{2j} |
|----------------------|----------------|----------------|----------------|----------------|----------------|---------------|---------------|
| medication errors | 5 | 2.5 | 53,373,000 | 20,000,000 | 16,000,000 | 1 | 1 |
| Ventilator failure | 4 | 80 | 2,393,000 | 14,500,000 | 15,000,000 | 1 | 0 |

The values of the statistical criterion were then obtained through intensive simulation studies. The number of repetitions was 10,000 to reduce inaccuracy in the simulation research. For a unique alternative, the ARL_0 values are calculated without any shift. However, the ARL_1 values are computed when the mean survival time decreases because of the incidence of the assignable cause linked to medication errors or ventilator failure, respectively. Figure 1 depicts the algorithm for computing the ARL_0 and ARL_1 of the risk-adjusted EWMA chart.

In the algorithm presented in Figure 1, first, a new value is defined for LCL and ν , and where the run length is equal to 0, the first iteration is started, and the statistics of the EWMA chart are adjusted for the initial values. Then, under in-control conditions, a patient is entered into the process, for which the value of risk factors and survival time are measured, and the statistics of the EWMA chart are updated. According to the patient's entry, the value of one must be added to the run length; otherwise, another patient must be entered into the process until the value of one is added to the run length. In this situation, the first iteration ends. This process is executed for 10,000 iterations, and the average length of the obtained sequences shows the value of ARL_0 . To determine the value of ARL_1 , it is treated similarly to the above steps, with the difference that patients in out-of-control conditions must be entered into the process.

Subsequently, to avoid having a signal when the process is in-control, and to receive a quick alarm when the process is out-of-control, the two statistical constraints were considered: $ATS_0(D) \geq 240$, and $ATS_{1j}(D) \leq 60$.

Therefore, the estimated time cost of using the suggested risk-adjusted EWMA chart in the healthcare above system could be determined. Because of the properties of the suggested MODM model and the successful operation of MOPSO, the set of non-dominated solutions was initially identified utilizing the stated technique. In other words, the MOPSO implementation with 500 replications, n -pop of size 100, $coe_1 = 2$ and $coe_2 = 2$, number of grids = 30, and $wc = 0.5$ were used to determine the optimal Pareto solutions. Forty solutions were chosen as non-dominated ones using the MOPSO. Table 5 and Figure 2 present the findings.

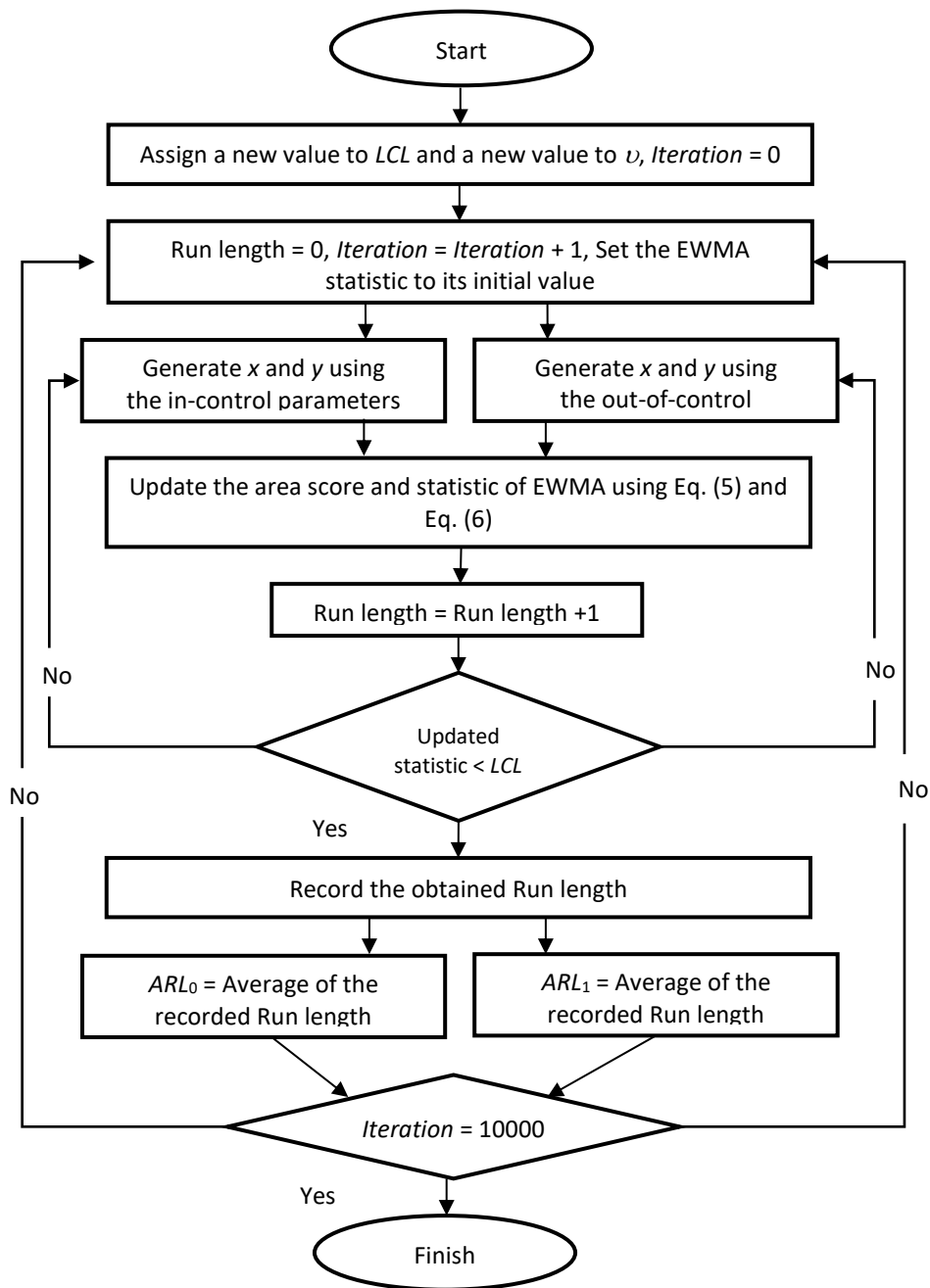


Fig. 1. The algorithm for computing the LCL , ARL_0 and ARL_1

Table 5
 Non-dominated solutions from the proposed multi-objective design model

| Design parameters | | Objective function | | |
|-------------------|-------|------------------------|------------------------|------------------------|
| <i>LCL</i> | ν | <i>Exp_A</i> | <i>ATS₀</i> | <i>ATS₁</i> |
| -0.41 | 0.01 | 3,683,789.50 | 1610.33 | 55.33 |
| -0.42 | 0.01 | 3,714,927.32 | 1618.66 | 56.27 |
| -0.47 | 0.01 | 3,718,993.87 | 1621.32 | 56.39 |
| -0.60 | 0.01 | 3,738,711.27 | 1690.97 | 57.00 |
| -0.62 | 0.01 | 3,738,240.20 | 1649.12 | 56.98 |
| -0.89 | 0.01 | 3,795,005.43 | 1732.98 | 58.73 |
| -1.07 | 0.01 | 3,798,251.89 | 1801.42 | 58.83 |
| -0.26 | 0.02 | 3,305,949.88 | 1019.68 | 44.49 |
| -0.43 | 0.02 | 3,331,907.86 | 1061.62 | 45.20 |
| -0.66 | 0.02 | 3,309,812.76 | 1056.76 | 44.59 |
| -0.70 | 0.02 | 3,344,844.94 | 1097.52 | 45.56 |
| -0.79 | 0.02 | 3,339,840.66 | 1091.02 | 45.42 |
| -0.84 | 0.02 | 3,380,904.69 | 1146.94 | 46.56 |
| -0.90 | 0.02 | 3,364,582.39 | 1125.86 | 46.10 |
| -1.01 | 0.02 | 3,396,215.20 | 1175.41 | 46.98 |
| -1.19 | 0.02 | 3,397,717.22 | 1188.54 | 47.02 |
| -1.27 | 0.02 | 3,417,319.33 | 1192.80 | 47.57 |
| -1.33 | 0.02 | 3,433,551.31 | 1259.51 | 48.03 |
| -1.35 | 0.02 | 3,430,020.96 | 1245.59 | 47.93 |
| -1.37 | 0.02 | 3,421,543.59 | 1231.69 | 47.69 |
| -1.43 | 0.02 | 3,451,874.68 | 1273.48 | 48.55 |
| -0.46 | 0.03 | 3,206,022.32 | 854.44 | 41.79 |
| -1.02 | 0.03 | 3,245,188.42 | 928.97 | 42.84 |
| -1.17 | 0.03 | 3,265,870.84 | 972.19 | 43.40 |
| -1.28 | 0.03 | 3,259,566.29 | 968.87 | 43.23 |
| -1.33 | 0.03 | 3,288,123.15 | 1011.27 | 44.00 |
| -1.34 | 0.03 | 3,271,412.37 | 998.80 | 43.55 |
| -0.30 | 0.04 | 3,135,747.45 | 701.15 | 39.93 |
| -0.66 | 0.04 | 3,142,981.22 | 714.80 | 40.12 |
| -0.68 | 0.04 | 3,155,860.06 | 758.24 | 40.46 |
| -0.74 | 0.04 | 3,167,788.80 | 759.63 | 40.78 |
| -0.86 | 0.04 | 3,168,743.40 | 773.90 | 40.80 |
| -1.35 | 0.04 | 3,212,052.11 | 874.31 | 41.95 |
| -0.36 | 0.05 | 3,114,475.05 | 617.92 | 39.38 |
| -0.55 | 0.05 | 3,114,889.62 | 664.59 | 39.39 |
| -1.05 | 0.05 | 3,151,434.73 | 717.68 | 40.35 |
| -1.44 | 0.05 | 3,178,866.37 | 821.75 | 41.07 |
| -0.40 | 0.06 | 3,096,608.48 | 576.88 | 48.91 |

| Design parameters | | Objective function | | |
|-------------------|-------|------------------------|------------------------|------------------------|
| <i>LCL</i> | ν | <i>Exp_A</i> | <i>ATS₀</i> | <i>ATS₁</i> |
| -0.66 | 0.06 | 3,104,651.23 | 610.56 | 39.12 |
| -0.64 | 0.07 | 3,103,219.50 | 578.84 | 39.09 |

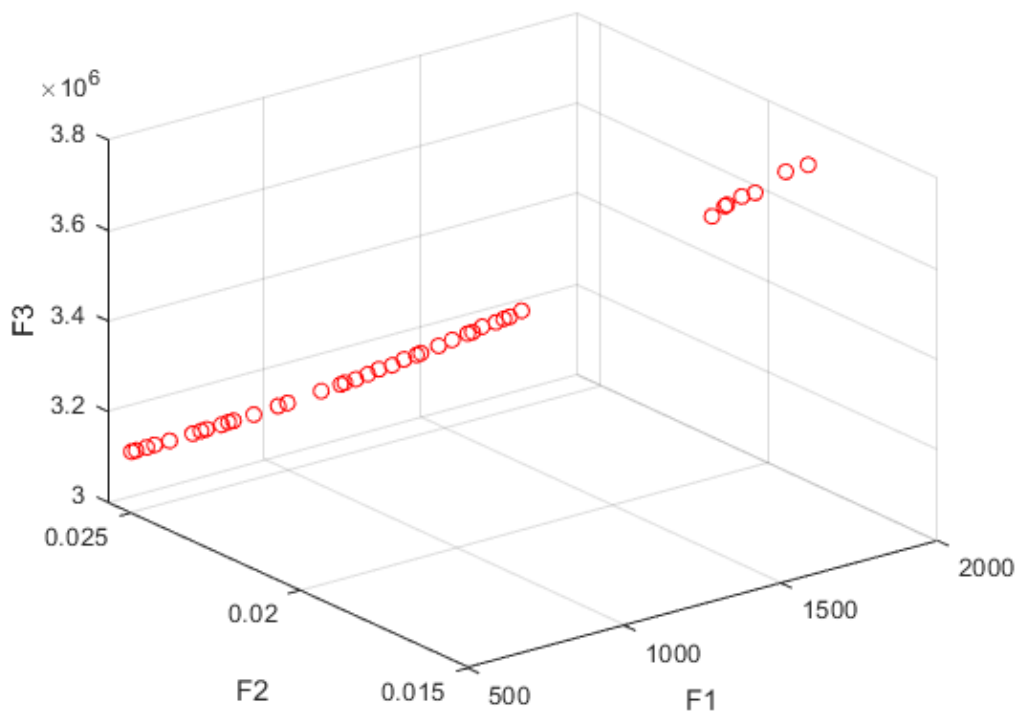


Fig. 2. Pareto front for $F1 = ATS_0$, $F2 = 1/ATS_1$ and $F3 = Exp_A$

Figure 2 shows that in the space of two parameters, LCL from -0.75 to -0.01 and ν from 0.01 to 0.2 , there are only forty combinations of (LCL, ν) whose solutions are better than those of other combinations. As mentioned earlier, the solutions for each combination of parameters are ATS_0 , $1/ATS_1$, and Exp_A . In addition, drawing these forty solutions on the Pareto frontier shows that they have no absolute superiority over each other and are identified as non-dominated solutions.

The VIKOR method was used to optimize the non-dominated (Pareto) solutions. Hence, the initial decision matrix was formed based on the information in Table 5, in which the design parameters were considered alternatives, and the three objective functions were considered evaluation criteria. In this matrix, the two criteria of Exp_A and ATS_1 were negative. Then, the criteria' ideal and negative ideal values were determined from Table 5 using Eq. (14) and Eq. (15) shown in Table 6.

Table 6

Values of ideal and negative ideal

| Ideal and Negative Ideal | Exp_A | ATS_0 | ATS_1 |
|--------------------------|--------------|---------|---------|
| Ideal | 3,096,608.48 | 1801.42 | 38.92 |
| Negative Ideal | 3,798,251.89 | 576.88 | 58.83 |

In the next stages, the values of the ideal and the negative ideal of criteria were utilized for calculating the utility measure (ut_i), regret measure (re_i), and the VIKOR index (Ω_i) using Eq. (16), Eq. (17), and Eq. (18). Table 7 is a list of the conclusions of these computations. In this study, the importance of cost function and statistical properties were considered equal to 0.333 from the healthcare experts' perspective. Also, the value of ξ was considered to be 0.5 .

Table 7
 Utility measure, regret measure and VIKOR index

| Alternatives (LCL, v) | Criteria | | |
|------------------------------|----------|-------|----------|
| | ut | re | Ω |
| (-0.41, 0.01) | 0.605 | 0.279 | 0.740 |
| (-0.42, 0.01) | 0.633 | 0.293 | 0.821 |
| (-0.47, 0.01) | 0.637 | 0.295 | 0.831 |
| (-0.60, 0.01) | 0.637 | 0.305 | 0.858 |
| (-0.62, 0.01) | 0.648 | 0.305 | 0.873 |
| (-0.89, 0.01) | 0.681 | 0.331 | 0.996 |
| (-1.07, 0.01) | 0.666 | 0.333 | 0.978 |
| (-0.26, 0.02) | 0.405 | 0.213 | 0.274 |
| (-0.43, 0.02) | 0.418 | 0.201 | 0.259 |
| (-0.66, 0.02) | 0.399 | 0.203 | 0.236 |
| (-0.70, 0.02) | 0.420 | 0.191 | 0.235 |
| (-0.79, 0.02) | 0.417 | 0.193 | 0.236 |
| (-0.84, 0.02) | 0.441 | 0.178 | 0.226 |
| (-0.90, 0.02) | 0.431 | 0.184 | 0.229 |
| (-1.01, 0.02) | 0.447 | 0.170 | 0.214 |
| (-1.19, 0.02) | 0.445 | 0.167 | 0.201 |
| (-1.27, 0.02) | 0.462 | 0.166 | 0.222 |
| (-1.33, 0.02) | 0.460 | 0.160 | 0.202 |
| (-1.35, 0.02) | 0.460 | 0.158 | 0.198 |
| (-1.37, 0.02) | 0.456 | 0.155 | 0.183 |
| (-1.43, 0.02) | 0.473 | 0.169 | 0.246 |
| (-0.46, 0.03) | 0.358 | 0.258 | 0.333 |
| (-1.02, 0.03) | 0.373 | 0.237 | 0.298 |
| (-1.17, 0.03) | 0.381 | 0.226 | 0.276 |
| (-1.28, 0.03) | 0.376 | 0.226 | 0.271 |
| (-1.33, 0.03) | 0.391 | 0.215 | 0.260 |
| (-1.34, 0.03) | 0.379 | 0.218 | 0.252 |
| (-0.30, 0.04) | 0.335 | 0.299 | 0.418 |
| (-0.66, 0.04) | 0.338 | 0.295 | 0.411 |
| (-0.68, 0.04) | 0.338 | 0.284 | 0.378 |
| (-0.74, 0.04) | 0.348 | 0.283 | 0.392 |
| (-0.86, 0.04) | 0.345 | 0.279 | 0.377 |
| (-1.35, 0.04) | 0.358 | 0.252 | 0.318 |
| (-0.36, 0.05) | 0.338 | 0.322 | 0.486 |
| (-0.55, 0.05) | 0.326 | 0.309 | 0.433 |
| (-1.05, 0.05) | 0.345 | 0.295 | 0.419 |
| (-1.44, 0.05) | 0.342 | 0.266 | 0.335 |
| (-0.40, 0.06) | 0.333 | 0.333 | 0.510 |
| (-0.66, 0.06) | 0.331 | 0.324 | 0.482 |
| (-0.64, 0.07) | 0.339 | 0.332 | 0.516 |
| <i>weight</i> | 0.333 | 0.333 | 0.333 |

The alternative solution with the lower VIKOR index was identified as the optimal solution in the VIKOR method's sixth stage. The ranking was then expanded following the increasing order of the VIKOR index. The ranking of the design parameters based on Ω_i , ut_i , and re_i is presented in Table 8.

Table 8

Ranking of the alternatives based on VIKOR index, utility measure, and regret measure

| Alternatives (LCL, v) | Ranking | | |
|------------------------------|---------|------|----------|
| | ut | re | Ω |
| (-0.41, 0.01) | 34 | 34 | 23 |
| (-0.42, 0.01) | 35 | 35 | 27 |
| (-0.47, 0.01) | 36 | 36 | 29 |
| (-0.60, 0.01) | 37 | 37 | 33 |
| (-0.62, 0.01) | 38 | 38 | 32 |
| (-0.89, 0.01) | 40 | 40 | 37 |
| (-1.07, 0.01) | 39 | 39 | 39 |
| (-0.26, 0.02) | 17 | 21 | 14 |
| (-0.43, 0.02) | 14 | 23 | 12 |
| (-0.66, 0.02) | 10 | 20 | 13 |
| (-0.70, 0.02) | 9 | 24 | 10 |
| (-0.79, 0.02) | 11 | 22 | 11 |
| (-0.84, 0.02) | 7 | 26 | 8 |
| (-0.90, 0.02) | 8 | 25 | 9 |
| (-1.01, 0.02) | 5 | 28 | 7 |
| (-1.19, 0.02) | 3 | 27 | 5 |
| (-1.27, 0.02) | 6 | 32 | 4 |
| (-1.33, 0.02) | 4 | 30 | 3 |
| (-1.35, 0.02) | 2 | 31 | 2 |
| (-1.37, 0.02) | 1 | 29 | 1 |
| (-1.43, 0.02) | 12 | 33 | 6 |
| (-0.46, 0.03) | 21 | 13 | 21 |
| (-1.02, 0.03) | 19 | 15 | 19 |
| (-1.17, 0.03) | 18 | 18 | 17 |
| (-1.28, 0.03) | 16 | 16 | 18 |
| (-1.33, 0.03) | 15 | 19 | 15 |
| (-1.34, 0.03) | 13 | 17 | 16 |
| (-0.30, 0.04) | 27 | 4 | 31 |
| (-0.66, 0.04) | 26 | 6 | 30 |
| (-0.68, 0.04) | 24 | 5 | 26 |
| (-0.74, 0.04) | 25 | 12 | 25 |
| (-0.86, 0.04) | 23 | 11 | 24 |
| (-1.35, 0.04) | 20 | 14 | 20 |
| (-0.36, 0.05) | 31 | 7 | 35 |
| (-0.55, 0.05) | 29 | 1 | 34 |
| (-1.05, 0.05) | 28 | 10 | 28 |
| (-1.44, 0.05) | 22 | 9 | 22 |
| (-0.40, 0.06) | 32 | 3 | 40 |
| (-0.66, 0.06) | 30 | 2 | 36 |
| (-0.64, 0.07) | 33 | 8 | 38 |

Finally, in step 7 of the VIKOR method, the validation of the ranking results was examined. For Condition 1, the solution (-1.37, 0.02) is the first design parameters according to Ω index, and the solution (-1.37, 0.02) is the first design parameters according to re measure. According to this result, Condition 1 is valid. For Condition 2, there is a calculation depending on the difference of Ω values of the first position in the ranking list and the second position in the ranking list and the number of alternatives. Thus, based on Eq. (19):

$$\Omega(A^1) = 0.183, \quad \Omega(A^2) = 0.198, \quad \Omega(A^3) = 0.201,$$

$$\Omega(A^4) = 0.202, \quad \Omega(A^5) = 0.214, \quad M = 40, \quad \text{and}$$

$$0.198 - 0.183 < 0.026,$$

$$0.201 - 0.183 < 0.026,$$

$$0.202 - 0.183 < 0.026,$$

$$0.214 - 0.183 \geq 0.026.$$

According to this result, Condition 2 is also invalid. As a result, four solutions (-1.37, 0.02), (-1.35, 0.02), (-1.33, 0.02), and (-1.01, 0.02) are considered to be the optimal design parameters of the risk-adjusted EWMA control chart in the surgical process and recovery of cardiovascular patients. Finally, according to the preferences of the decision-makers of the study case, among the optimal solutions, the solution with the lowest cost was selected, i.e., ($LCL = -1.01$, $\nu = 0.02$) with $Exp_A = 3,396,215.20$ Rials, $ATS_0 = 1175.41$ and $ATS_1 = 46.98$. As a result, the risk-adjusted EWMA created using the above parameters combines the most favorable statistical and economic considerations.

7. Comparison of the Proposed Multiple-Objective Model with Single-Objective Model

This part compared the single-objective (economic) model and the proposed ESD model of the risk-adjusted EWMA control chart. It should be emphasized that for performance evaluation, both the pure and the proposed models with statistical aspects are investigated. The ideal parameters for three competing models are shown in Table 9. The ATS_0 has improved by roughly 51% compared to the pure economic model, but the ATS_1 has seen no significant improvement. In contrast, the Exp_A has increased up to 8%. This demonstrates that the statistical performance of the risk-adjusted EWMA control chart might be greatly enhanced by applying the ESD approach, with just a slight increase in cost. Interestingly, the single objective economic model with statistical properties cannot compete with the suggested MODM design model.

Table 9
 A comparison of multi-objective and single-objective design model

| Design | (LCL, ν) | ATS_0 | ATS_1 | Exp_A (Rials) |
|-----------------------|----------------|---------|---------|-----------------|
| Multi-objective model | (-1.01, 0.02) | 1175.41 | 46.98 | 3,396,215.20 |
| Pure economic model | (-0.40, 0.06) | 576.88 | 48.91 | 3,096,608.48 |

8. Conclusion

To manage the surgical process and recovery of cardiovascular patients effectively, the economic-statistical design of the risk-adjusted EWMA chart with various objectives was examined. The risk-adjusted EWMA chart was used to explore downward shifts in the survival times of cardiovascular patients. The AFT, a well-known risk-adjusted regression model, was used to successfully account for the impact of risk variables on the patients' survival times. A multi-objective design model was then developed by taking into account the expected cost function (Exp_A), the average time to signal when the process is under control (ATS_0), and the average time to signal when the process is out of control (ATS_1). The suggested MODM model includes several assignable causes with various occurrence rates and consequences during the surgical procedure.

Given that the sample size and sampling interval remained constant throughout the process, (LCL, ν) was chosen as the optimal design parameter. The optimal design parameters were then provided using a two-stage ranking evaluation process with the MOPSO and VIKOR parameters. The suggested

MODM model was used in an actual case study at the government hospital for cardiovascular patients with two unique assignable causes by the provided solution algorithm. The proposed multi-objective model and single-objective models were then compared for performance. Based on the analysis, the following conclusions can be drawn:

- The MOPSO algorithm accurately identified 40 non-dominated solutions out of a large set of solutions.
- The VIKOR technique could accurately rank non-dominated solutions based on the Exp_A , ATS_0 , and ATS_1 criteria.
- To use the risk-adjusted EWMA control chart, the LCL and U parameters should be set to -1.01 and 0.02, respectively.
- Using the risk-adjusted EWMA control chart with selected parameters, with Exp_A equal to 3,396,215.20, ATS_0 equal to 1175.41, and ATS_1 equal to 46.98, is the best economic-statistical design of the risk-adjusted EWMA control chart.
- The results unequivocally show that the multi-objective design outperforms the pure economic model when statistical constraints are considered, as it increases the statistical properties by 51% with a slight increase in the cost amount.

Thus, the suggested method for creating the risk-adjusted EWMA chart may be effectively used to detect shifts in the decreasing survival time of cardiovascular patients within healthcare systems.

Finally, an exciting area worthy of continued research is to compare the results obtained here with other methods used to construct control charts, such as non-parametric approaches. In addition, it is essential to categorize the assignable causes into different groups based on their ability to shift the mean survival time, which can be small, moderate, or large. Using the fuzzy set theory to represent the severity of each category could be an exciting approach. How to incorporate the correlation while using the AFT regression models is a potentially helpful area for future research. Another attractive research area for future research involves investigating and comparing methods other than MOPSO and VIKOR to solve the multi-objective model.

Author Contributions

Conceptualization, A.N.P and A.A.; methodology, A.N.P. and M.J.E.; software, A.R.; validation, A.N.P., A.A. and A.R.; formal analysis, M.J.R.; investigation, M.Z.; resources, A.A. and M.J.E.; data curation, A.R.; writing—original draft preparation, A.N.P.; writing—review and editing, A.N.P. and M.Z.; visualization, M.J.E.; supervision, A.A.; project administration, M.J.E. All authors have read and agreed to the published version of the manuscript.

Funding

This research received no external funding.

Data Availability Statement

The authors confirm that the data supporting the findings of this study are available within the article.

Conflicts of Interest

The authors declare that they have no known competing financial interests or personal relationships that could have appeared to influence the work reported in this paper.

Acknowledgement

The authors express their appreciation and gratitude for the support of the Vice-Chancellor for Research and Technology of Kermanshah, University of Medical Science.

References

- [1] Yeganeh, A., Shadman, A., Shongwe, S. C., & Abbasi, S. A. (2023). Employing evolutionary artificial neural network in risk-adjusted monitoring of surgical performance. *Neural Computing and Applications*, 35(14), 10677-10693. <https://doi.org/10.1007/s00521-023-08257-x>
- [2] Mustafa, F., Sherwani, R. A. K., & Raza, M. A. (2023). A new exponentially weighted moving average control chart to monitor count data with applications in healthcare and manufacturing. *Journal of Statistical Computation and Simulation*, 93(18), 3308-3328. <https://doi.org/10.1080/00949655.2023.2220859>
- [3] Duncan, A. J. (1956). The economic design of X charts used to maintain current control of a process. *Journal of the American statistical association*, 51(274), 228-242. <https://doi.org/10.1080/01621459.1956.10501322>
- [4] Lorenzen, T. J., & Vance, L. C. (1986). The economic design of control charts: a unified approach. *Technometrics*, 28(1), 3-10. <https://doi.org/10.2307/1269598>
- [5] Serel, D. A. (2009). Economic design of EWMA control charts based on loss function. *Mathematical and Computer Modelling*, 49(3-4), 745-759. <https://doi.org/10.1016/j.mcm.2008.06.012>
- [6] Lu, S. L., & Huang, C. J. (2017). Statistically constrained economic design of maximum double EWMA control charts based on loss functions. *Quality Technology & Quantitative Management*, 14(3), 280-295. <https://doi.org/10.1080/16843703.2016.1208940>
- [7] Xue, L., Wang, Q., Li, C., & An, L. (2023). Economic design of residuals MEWMA control chart with variable sampling intervals and sample size. *Communications in Statistics-Simulation and Computation*, 1-22. <https://doi.org/10.1080/03610918.2023.2257008>
- [8] Rafiei, N., Asadzadeh, S., & Niaki, S. T. A. (2021). Multi-objective design of risk-adjusted control chart in healthcare systems with economic and statistical considerations. *Communications in Statistics-Simulation and Computation*, 52(7), 2667-2984. <https://doi.org/10.1080/03610918.2021.1923744>
- [9] Saniga, E. M. (1989). Economic statistical control-chart designs with an application to and R charts. *Technometrics*, 31(3), 313-320. <https://doi.org/10.2307/3556141>
- [10] Niaki, S. T. A., Malaki, M., & Ershadi, M. J. (2011). A particle swarm optimization approach on economic and economic-statistical designs of MEWMA control charts. *Scientia Iranica*, 18(6), 1529-1536. <https://doi.org/10.1016/j.scient.2011.09.007>
- [11] Amiri, A., Moslemi, A., & Doroudyan, M. H. (2015). Robust economic and economic-statistical design of EWMA control chart. *The International Journal of Advanced Manufacturing Technology*, 78, 511-523. <https://doi.org/10.1007/s00170-014-6667-9>
- [12] Katebi, M., & Pourtaheri, R. (2019). An economic statistical design of the Poisson EWMA control charts for monitoring nonconformities. *Journal of Statistical Computation and Simulation*, 89(15), 2813-2830. <https://doi.org/10.1080/00949655.2019.1638390>
- [13] Lee, M. H., Khoo, M. B., Haq, A., & Chew, X. (2023). Economic-statistical design of the variable sampling interval Poisson EWMA chart. *Communications in Statistics-Simulation and Computation*, 52(5), 2139-2150. <https://doi.org/10.1080/03610918.2021.1898637>
- [14] Rafiei, N., & Asadzadeh, S. (2022). Designing a risk-adjusted CUSUM control chart based on DEA and NSGA-II approaches A case study in healthcare: Cardiovascular patients. *Scientia Iranica*, 29(5), 2696-2709. <https://doi.org/10.24200/SCI.2020.54743.3895>
- [15] Sego, L. H., Reynolds Jr, M. R., & Woodall, W. H. (2009). Risk-adjusted monitoring of survival times. *Statistics in medicine*, 28(9), 1386-1401. <https://doi.org/10.1002/sim.3546>
- [16] Mohammadian, F., Niaki, S. T. A., & Amiri, A. (2016). Phase-I risk-adjusted geometric control charts to monitor health-care systems. *Quality and Reliability Engineering International*, 32(1), 19-28. <https://doi.org/10.1002/qre.1722>
- [17] Begun, A., Kulinskaya, E., & MacGregor, A. J. (2019). Risk-adjusted CUSUM control charts for shared frailty survival models with application to hip replacement outcomes: a study using the NJR dataset. *BMC medical research methodology*, 19(1), 1-15. <https://doi.org/10.1186/s12874-019-0853-2>
- [18] Kim, J. S., Choi, M., Kim, S. H., Choi, S. H., & Kang, C. M. (2022). Safety and feasibility of laparoscopic pancreaticoduodenectomy in octogenarians. *Asian Journal of Surgery*, 45(3), 837-843. <https://doi.org/10.1016/j.asjsur.2021.09.021>
- [19] Yeganeh, A., Chukhrova, N., Johannssen, A., & Fotuhi, H. (2023). A network surveillance approach using machine learning based control charts. *Expert Systems with Applications*, 219, 119660. <https://doi.org/10.1016/j.eswa.2023.119660>
- [20] Ghaseminejad, A., Kazemipoor, H., & Fallah, M. (2023). Modeling the robust facility layout problem for unequal space considering health and environmental safety criteria under uncertain parameters. *Decision Making: Applications in Management and Engineering*, 6(2), 426-460. <https://doi.org/10.31181/dmame622023607>

- [21] Mohammad, N. E. G., Rawash, Y. Y., Aly, S. M., Awad, M. E. S., & Mohamed, M. H. H. (2023). Enhancing gas pipeline network efficiency through VIKOR method. *Decision Making: Applications in Management and Engineering*, 6(2), 853-879. <https://doi.org/10.31181/dmame622023868>
- [22] Saraji, M. K., Aliasgari, E., & Streimikiene, D. (2023). Assessment of the challenges to renewable energy technologies adoption in rural areas: A Fermatean CRITIC-VIKOR approach. *Technological Forecasting and Social Change*, 189, 122399. <https://doi.org/10.1016/j.techfore.2023.122399>
- [23] Liang, W. Z., Zhao, G. Y., & Hong, C. S. (2018). Performance assessment of circular economy for phosphorus chemical firms based on VIKOR-QUALIFLEX method. *Journal of Cleaner Production*, 196, 1365-1378. <https://doi.org/10.1016/j.jclepro.2018.06.147>
- [24] Knoth, S., Wittenberg, P., & Gan, F. F. (2019). Risk-adjusted CUSUM charts under model error. *Statistics in medicine*, 38(12), 2206-2218. <https://doi.org/10.1002/sim.8104>
- [25] Parsa, M., & Van Keilegom, I. (2023). Accelerated failure time vs Cox proportional hazards mixture cure models: David vs Goliath?. *Statistical Papers*, 64(3), 835-855. <https://doi.org/10.1007/s00362-022-01345-5>
- [26] Ding, N., He, Z., Shi, L., & Qu, L. (2021). A new risk-adjusted EWMA control chart based on survival time for monitoring surgical outcome quality. *Quality and Reliability Engineering International*, 37(4), 1650-1663. <https://doi.org/10.1002/qre.2818>
- [27] Liu, L., Lai, X., Zhang, J., & Tsung, F. (2018). Online profile monitoring for surgical outcomes using a weighted score test. *Journal of Quality Technology*, 50(1), 88-97. <https://doi.org/10.1080/00224065.2018.1404329>
- [28] Ganguly, S. (2020). Multi-objective distributed generation penetration planning with load model using particle swarm optimization. *Decision Making: Applications in Management and Engineering*, 3(1), 30-42. <https://doi.org/10.31181/dmame2003065g>
- [29] Tavana, M., Li, Z., Mobin, M., Komaki, M., & Teymourian, E. (2016). Multi-objective control chart design optimization using NSGA-III and MOPSO enhanced with DEA and TOPSIS. *Expert Systems with Applications*, 50, 17-39. <https://doi.org/10.1016/j.eswa.2015.11.007>
- [30] Yildirim, B. F., & Yildirim, S. K. (2022). Evaluating the satisfaction level of citizens in municipality services by using picture fuzzy VIKOR method: 2014-2019 period analysis. *Decision Making: Applications in Management and Engineering*, 5(1), 50-66. <https://doi.org/10.31181/dmame181221001y>